nearly identical. We have noted that the barriers are approximately 0.5 V different in height, which is probably a large fraction of their total height. If the barriers were the rate-limiting step in the tunneling process, one would expect a very strong asymmetry in the characteristic on this account. The symmetry of the characteristic is strong evidence that the current is bulk controlled rather than electrode controlled.

Another rather conclusive evidence for the bulk process is in the voltage required for a given current in the forward and reverse directions. Plotted in Fig. 11 are the forward and reverse voltages for a number of units of different thicknesses. The straight line with unity slope and intercept at twice the difference in work functions is to be expected from a bulk field ionization process. The curve for electrode tunneling would be steeper by the ratio of the barrier heights.

The value of V as calculated from Fig. 10 is about twice that obtained from the temperature data in Fig. 9 but detailed comparison is difficult due to the uncertainties in m^* and V_g in Eq. (2).

CONCLUSIONS

This author can see no way in which the usual electrode-controlled processes can be made to explain the observed experimental characteristics. Although all of the work reported here has been done with tantalum oxide films, many other films exhibit very similar characteristics and the above considerations undoubtedly apply in some cases. It should be emphasized that with the experimental evidence at hand, it is impossible to establish a complete model of the current flow processes in these films. However, it is believed that the mechanisms proposed are the rate-limiting processes involved and should be carefully considered in the construction of any complete analysis.

ACKNOWLEDGMENTS

The author is indebted to H. M. Simpson who fabricated most of the diodes used in these experiments. Thanks are also due R. Stratton, A. Rose, C. Wilts, and H. Sommers, for helpful discussions and criticisms.

PHYSICAL REVIEW VOLUME 128, NUMBER 5 DECEMBER 1, 1962

Wave-Number-Dependent Dielectric Function of Semiconductors*

DAVID R. PENN
Physics Department and Institute for the Study of Metals, University of Chicago, Chicago, Illinois
(Received April 2, 1962; revised manuscript received August 17, 1962)

Expressions for the wave-number-dependent dielectric function are derived for various models of a semiconductor. The calculation is carried out for the diagonal part of the dielectric function at zero frequency. It is found that calculations based on plane wave models (such as the free electron model) give poor results for small values of the wave number due to neglect of both Bragg reflections and Umklapp processes. We use instead an isotropic version of the nearly free electron model in which dielectric function depends on only one parameter E_g representing an average energy gap that can be determined from optical data. It is noted that for small wave numbers Umklapp processes give the major contribution to the dielectric function, whereas for large wave numbers normal processes dominate. The dielectric function is evaluated numerically for a value of E_g appropriate to Si.

I. INTRODUCTION

THE interaction between an external electric field and the electrons in a solid can be described by the relationship

$$V(\mathbf{r},t)=\int\int \mathcal{K}(\mathbf{r},\mathbf{r}';t-t')V_{\text{ext}}(\mathbf{r}',t')d\mathbf{r}'dt',$$

where V_{ext} is the potential due to the external field, V is the total microscopic potential, and $\mathcal{K}$ describes the response of the solid to V_{ext}. For the case of a solid with a periodic lattice we can write

$$\mathcal{K}(\mathbf{r},\mathbf{r}',t-t')=\int\int d\omega d\mathbf{q}\sum_{\mathbf{K}}\mathcal{K}(\mathbf{q},\mathbf{q}+\mathbf{K};\omega)e^{i\mathbf{q}\cdot(\mathbf{r}-\mathbf{r}')-i\mathbf{K}\cdot\mathbf{r}'-i\omega(t-t')},$$

where $\mathbf{K}$ is a reciprocal lattice vector. A general discussion of the inverse dielectric function, $\mathcal{K}$, has been given by Falk.[1]

The formalism can be used to treat the screened electron-electron interaction in the crystal by letting V_{ext} be the coulomb potential of the electron in the solid. Hubbard[2] has used the dielectric function to derive expressions for the ground-state energy of a medium, Quinn and Ferrell[3] have shown how $\mathcal{K}$ can be used in computing quasi-particle energies, and Phillips[4] has shown how it can be employed in forming a screened exchange operator.

Calculating $\mathcal{K}(\mathbf{q},\mathbf{q}+\mathbf{K};\omega)$ for arbitrary $\mathbf{K}$ and ω is generally very difficult. However, under certain circum-

* Supported in part by the National Science Foundation.

[1] D. Falk, Phys. Rev. **118**, 105 (1960).
[2] J. Hubbard, Proc. Roy. Soc. **A244**, 199 (1958).
[3] J. J. Quinn and R. A. Ferrell, Phys. Rev. **112**, 812 (1958).
[4] J. C. Phillips, Phys. Rev. **123**, 420 (1961).

stances, we need only consider values of $\mathcal{K}$ for which $\mathbf{K}$ or ω equal zero. In the case of a free electron gas, $\mathcal{K}$ vanishes for $K\neq 0$ due to the complete translational invariance of the system, and several authors[2,5] have derived expressions for $\mathcal{K}$. Phillips[4] has suggested that even for Si, which is characterized by strong covalent bonding, $\mathcal{K}(\mathbf{q}, \mathbf{q}+\mathbf{K}; \omega)$ is small compared with $\mathcal{K}(\mathbf{q},\mathbf{q}; \omega)$, and further, for the purpose of forming a screened exchange-potential, it is sufficient to set $\omega=0$.

In this paper we calculate $\mathcal{K}(\mathbf{q})\equiv\mathcal{K}(\mathbf{q},\mathbf{q}; 0)\equiv 1/\epsilon(\mathbf{q})$ for the case of a one-parameter model of a semiconductor. Our results shed light on the feasibility of calculating $\mathcal{K}$ for crystals having more complicated energy spectra than a free electron gas. Numerical results are given using the value of the parameter appropriate to Si.

II. DISCUSSION OF SEMICONDUCTOR MODELS

The expression for $\epsilon(\mathbf{q})$ is given by several authors,[6,7]

$$\epsilon(\mathbf{q})=1-(4\pi e^2/q^2)\sum_{\mathbf{k},l,l'}|\langle\mathbf{k}l|e^{-i\mathbf{q}\cdot\mathbf{r}}|\mathbf{k}+\mathbf{q},l'\rangle|^2\times\frac{N_{\mathbf{k}+\mathbf{q},l'}-N_{\mathbf{k}l}}{E_{\mathbf{k}+\mathbf{q},l'}-E_{\mathbf{k}l}},\quad(2.1)$$

where

$$\langle\mathbf{k}l|e^{-i\mathbf{q}\cdot\mathbf{r}}|\mathbf{k}+\mathbf{q},l'\rangle\equiv\int\psi_{\mathbf{k}l}^*(\mathbf{r})e^{-i\mathbf{q}\cdot\mathbf{r}}\psi_{\mathbf{k}+\mathbf{q},l'}(\mathbf{r})d\mathbf{r}$$

and $N_{\mathbf{k}l}$ is the occupation number of the state $\mathbf{k}l$. The Bloch wave function $\psi_{\mathbf{k}l}(\mathbf{r})$, having reduced wave vector $\mathbf{k}$ and belonging to the band l, satisfies the equation

$$H_0\psi_{\mathbf{k}l}=E_{\mathbf{k}l}\psi_{\mathbf{k}l},$$

where H_0 is the one-electron Hamiltonian in the absence of V_{ext}.

For our purposes it is convenient to express (2.1) in the extended zone scheme,

$$\epsilon(\mathbf{q})=1+(4\pi e^2/q^2)\sum_{\mathbf{k},\mathbf{K}}|\langle\mathbf{k}|e^{-i\mathbf{q}\cdot\mathbf{r}}|\mathbf{k}+\mathbf{q}+\mathbf{K}\rangle|^2\times\frac{N_{\mathbf{k}+\mathbf{q}+\mathbf{K}}-N_{\mathbf{k}}}{E_{\mathbf{k}+\mathbf{q}+\mathbf{K}}-E_{\mathbf{k}}},\quad(2.2)$$

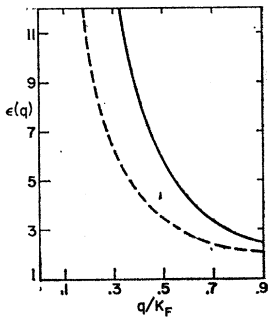

FIG. 1. Dielectric function vs wave number. The solid curve refers to the free electron model and the dashed curve refers to Callaway's model.

where $\mathbf{K}$ is a reciprocal lattice vector. The second term of (2.2) represents virtual transitions, induced by V_{ext}, between the states $\mathbf{k}$ and $\mathbf{k}+\mathbf{q}+\mathbf{K}$. Those transitions for which $\mathbf{K}=0$ are referred to as "normal" while those for which $\mathbf{K}\neq 0$ are termed "Umklapp."

Because dielectric screening involves all the valence electrons and hence is comparatively insensitive to details of the band structure, one would attempt to describe the screening on the basis of a relatively simple model. Two crude approximations to $\epsilon(\mathbf{q})$ may be suggested. If $\epsilon(0)$, the static dielectric constant, is much greater than unity, we may approximate $\epsilon(\mathbf{q})$ by its value for the free electron gas[2,4]:

$$\epsilon(\mathbf{q})=1+\tfrac{3}{8}(\hbar\omega_p/\bar{q}E_F)^2\times[1+(\bar{q}^{-1}-\tfrac{1}{4}\bar{q})\ln(|2+\bar{q}|/|2-\bar{q}|)],\quad(2.3)$$

where $\bar{q}\equiv q/K_F$, $\omega_p^2\equiv 4\pi Ne^2/m$; and E_F is the Fermi energy. A plot of $\epsilon(\mathbf{q})$ is shown in Fig. 1. A somewhat more refined approximation has been used by Callaway[8]

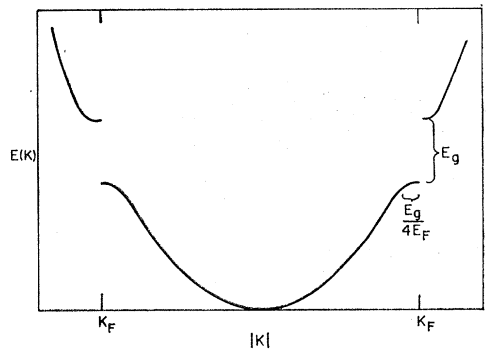

FIG. 2. Electron energy as a function of k for isotropic three-dimensional nearly free electron model.

who modified the above model by inserting an energy gap between the valence and conduction bands. The energy spectrum with the gap is

$$\begin{aligned}E_{\mathbf{k}}&=(\hbar^2/2m)k^2, &(k<K_F)\\ E_{\mathbf{k}}&=(\hbar^2/2m)k^2+E_g, &(k>K_F),\end{aligned}\quad(2.4)$$

where E_g is a parameter to be determined. For this model, (2.2) leads to

$$\epsilon(\mathbf{q})=1+\tfrac{3}{8}(\hbar\omega_p/E_F\bar{q})^2\Big\{1+\tfrac{1}{2}(\bar{E}/\bar{q})-(\bar{E}/\bar{q})[\ln|1+2(\bar{q}/\bar{E})-(\bar{q}^2/\bar{E})|]+\left(\frac{2-\bar{E}}{2\bar{q}}-\frac{\bar{q}}{4}-\frac{\bar{E}^2}{4\bar{q}^3}\right)\ln\frac{|2+\bar{q}+(\bar{E}/\bar{q})|}{|2-\bar{q}+(\bar{E}/\bar{q})|}\Big\},\quad(2.5)$$

where $\bar{E}=E_g/E_F$ and $\bar{q}=q/K_F$. A plot of $\epsilon(\mathbf{q})$ is shown in Fig. 1.

[5] J. Lindhard, Kgl. Danske Videnskab. Selskab, Mat.-fys. Medd. **28**, 8 (1954).
[6] P. Nozières and D. Pines, Phys. Rev. **109**, 762 (1958).
[7] H. Ehrenreich and M. H. Cohen, Phys. Rev. **115**, 786 (1959).
[8] J. Callaway, Phys. Rev. **116**, 1638 (1959).

The value of the parameter E_g which appears in Callaway's model should be determined by the condition that $\epsilon(0)$ as given by (2.5) be equal to the measured static dielectric constant. However, (2.5) gives an infinite value for $\epsilon(0)$ independent of E_g. This anomalous behavior occurs because this model does not allow for the formation of standing waves at the Brillouin zone boundaries. Moreover, the neglect of Umklapp processes leads to serious error.

For these reasons, we chose a different model, viz., the nearly free electron model, isotropically extended to three dimensions. This model is described by

$$E_{\mathbf{k}}^{\pm}=\tfrac{1}{2}\{E_{\mathbf{k}}^{0}+E_{\mathbf{k}'}^{0}\pm[(E_{\mathbf{k}}^{0}-E_{\mathbf{k}'}^{0})^2+E_g^2]^{1/2}\}, \quad (2.6)$$

$$\psi_{\mathbf{k}}=(e^{i\mathbf{k}\cdot\mathbf{r}}+\alpha_{\mathbf{k}}^{\pm}e^{i\mathbf{k}'\cdot\mathbf{r}})/[1+(\alpha_{\mathbf{k}}^{\pm})^2]^{1/2}, \quad (2.7)$$

where

$$\alpha_{\mathbf{k}}^{\pm}\equiv\tfrac{1}{2}E_g/(E_{\mathbf{k}}^{\pm}-E_{\mathbf{k}'}^{0}),$$
$$E_{\mathbf{k}}^{0}\equiv(\hbar^2/2m)k^2, \quad \mathbf{k}'\equiv\mathbf{k}-2K_F\hat{k},$$

and E_g is a parameter. The superscripts + and − on

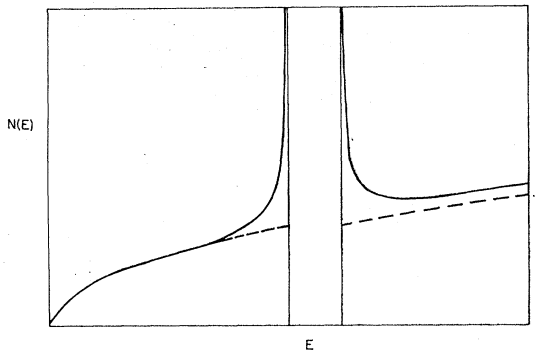

FIG. 3. Density of states vs energy. The solid curve refers to the three-dimensional nearly free electron model and the dashed curve refers to Callaway's model.

$E_{\mathbf{k}}^{\pm}$ refer to the cases $k>K_F$ and $k<K_F$, respectively. Figure 2 shows a graph of energy versus wave vector for this model. Figure 3 gives a plot of the density of states versus energy; our model removes states from the energy gap and piles them up at the top of the valence band and the bottom of the conduction band.

Unlike the two crude models, our model allows for the formation of standing waves at the zone edge and for the possibility of Umklapp processes. This will result in reasonable values of $\epsilon(\mathbf{q})$ for small values of $\mathbf{q}$, whereas, for q/K_F greater than unity, $\epsilon(\mathbf{q})$ is essentially the same for all three models.

Of course, our model is only a first approximation to a real semiconductor. We have replaced the actual rather complicated band structure by a much simpler one. Involved in this simplification is the neglect of degeneracies; these degeneracies sometimes occur at points in the Brillouin zone which are important in

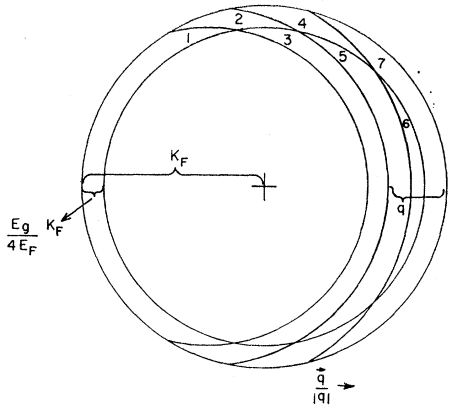

FIG. 4. Division of k space into sections for the purpose of computing $\epsilon(q)$.

determining optical properties. In spite of these shortcomings, we will see that our model gives a reasonable value for the parameter E_g in the cases of Si and Ge. We point out that the isotropy of our model suggests that it might also be applicable to a liquid or an amorphous semiconductor.

III. CALCULATION OF $\epsilon(\mathbf{q})$

For our model, (2.2) can be written as

$$\epsilon(\mathbf{q})=1+\frac{8\pi e^2}{q^2}\Big[\sum_{\mathbf{k}}N_{\mathbf{k}}(1-N_{\mathbf{k}+\mathbf{q}})\frac{|\langle\mathbf{k}|e^{-i\mathbf{q}\cdot\mathbf{r}}|\mathbf{k}+\mathbf{q}\rangle|^2}{E_{\mathbf{k}+\mathbf{q}}^{+}-E_{\mathbf{k}}^{-}}$$
$$+\sum_{\mathbf{k}}N_{\mathbf{k}}(1-N_{\mathbf{k}'})\frac{|\langle\mathbf{k}|e^{-i\mathbf{q}\cdot\mathbf{r}}|\mathbf{k}'\rangle|^2}{E_{\mathbf{k}'}^{+}-E_{\mathbf{k}}^{-}}\Big], \quad (3.1)$$

where $\mathbf{k}'\equiv\mathbf{k}+\mathbf{q}-(2K_F)(\mathbf{k}+\mathbf{q})/|\mathbf{k}+\mathbf{q}|$. Evaluation of the matrix elements gives

$$\langle\mathbf{k}|e^{-i\mathbf{q}\cdot\mathbf{r}}|\mathbf{k}+\mathbf{q}\rangle=(1+\alpha_{\mathbf{k}}^{-}\alpha_{\mathbf{k}+\mathbf{q}}^{+})/[1+(\alpha_{\mathbf{k}}^{-})^2]^{1/2}[1+(\alpha_{\mathbf{k}+\mathbf{q}}^{+})^2]^{1/2},$$
$$\langle\mathbf{k}|e^{-i\mathbf{q}\cdot\mathbf{r}}|\mathbf{k}'\rangle=(\alpha_{\mathbf{k}'}^{+}+\alpha_{\mathbf{k}}^{-})/[1+(\alpha_{\mathbf{k}}^{-})^2]^{1/2}[1+(\alpha_{\mathbf{k}'}^{+})^2]^{1/2}. \quad (3.2)$$

In order to evaluate the sums in (3.1) we introduce the following approximations for $E_{\mathbf{k}}^{\pm}$:

$$\begin{aligned}
&E_{\mathbf{k}}^{-}\approx(\hbar^2/2m)k^2, && (k/K_F<1-\tfrac{1}{4}\bar{E})\\
&E_{\mathbf{k}}^{-}\approx(\hbar^2/2m)(1-\tfrac{1}{4}\bar{E})^2K_F^2, && (1-\tfrac{1}{4}\bar{E}<k/K_F<1)\\
&E_{\mathbf{k}}^{+}\approx(\hbar^2/2m)(1+\tfrac{1}{4}\bar{E})^2K_F^2, && (1+\tfrac{1}{4}\bar{E}>k/K_F>1)\\
&E_{\mathbf{k}}^{+}\approx(\hbar^2/2m)k^2, && (1+\tfrac{1}{4}\bar{E}<k/K_F)
\end{aligned} \quad (3.3)$$

where again $\bar{E}=E_g/E_F$. These approximations consist of replacing the peaks shown in the density of states plot (Fig. 3) by delta functions. This will introduce an error in $\epsilon(\mathbf{q})$ that is of order E_g/E_F.

We now divide the Brillouin zone into sections as is

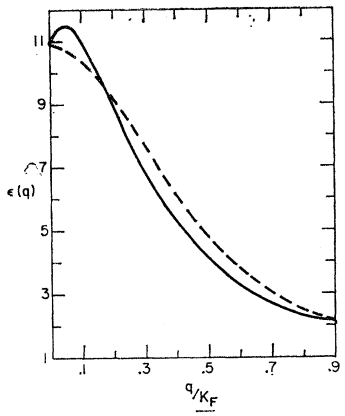

FIG. 5. Dielectric function vs wave number. The solid curve refers to our calculation and the dashed curve refers to an interpolation formula.

pictured in Fig. 4. Then, (3.1) can be written as

$$\epsilon(\mathbf{q})=1+\frac{8\pi e^2}{q^2}\sum_{\mathbf{k}i}\delta_{\mathbf{k}}{}^i\frac{|M_i|^2}{E_i}, \tag{3.4}$$

where $\delta_{\mathbf{k}}{}^i=1$ if $\mathbf{k}$ lies in region i and $\delta_{\mathbf{k}}{}^i=0$ otherwise, and M_i is the appropriate matrix element. The E_i are given by

$$E_1=(\hbar^2/2m)[\mathbf{k}'^2-(1-\tfrac{1}{4}\bar{E})^2K_F{}^2],\quad E_2=E_4=E_g,$$
$$E_3=E_5=(\hbar^2/2m)[(1+\tfrac{1}{4}\bar{E})^2K_F{}^2-\mathbf{k}^2],$$
$$E_6=(\hbar^2/2m)[(\mathbf{k}+\mathbf{q})^2-\mathbf{k}^2],$$
$$E_7=(\hbar^2/2m)[(\mathbf{k}+\mathbf{q})^2-(1-\tfrac{1}{4}\bar{E})^2K_F{}^2],$$

where $\mathbf{k}'\equiv\mathbf{k}+\mathbf{q}-2K_F(\mathbf{k}+\mathbf{q})/|\mathbf{k}+\mathbf{q}|$ and $\bar{E}=E_g/E_F$.

We shall next approximate the matrix elements by an interpolation formula. From (3.2) we find that $|\langle\mathbf{k}|e^{-i\mathbf{q}\cdot\mathbf{r}}|\mathbf{k}+\mathbf{q}\rangle|$ and $|\langle\mathbf{k}|e^{-i\mathbf{q}\cdot\mathbf{r}}|\mathbf{k}'\rangle|$ both approach $2E_F\mathbf{q}\cdot\mathbf{k}/E_gK_F$ as $q\to 0$. Using this result and the fact that we must get free electron behavior as $q\to\infty$ leads to

$$|\langle\mathbf{k}|e^{-i\mathbf{q}\cdot\mathbf{r}}|\mathbf{k}+\mathbf{q}\rangle|\approx|\langle\mathbf{k}|e^{-i\mathbf{q}\cdot\mathbf{r}}|\mathbf{k}'\rangle|$$
$$\approx(2qE_F/\sqrt{3}E_gK_F)^2[1+(2qE_F/\sqrt{3}E_gK_F)^2]^{-1}. \tag{3.5}$$

Combining (3.4) and (3.5) gives the final expression for $\epsilon(\mathbf{q})$ which is written out in the appendix.

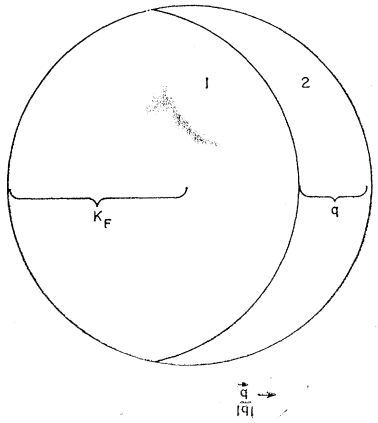

FIG. 6. The Fermi sphere is divided into two parts. Part 1 corresponds to the region in which Umklapp processes contribute to $\epsilon(q)$ while part 2 corresponds to the normal process.

TABLE I. Contributions to ϵ as a function of q/K_F. ϵ_1 and ϵ_2 are the contributions to ϵ arising from regions 1 and 2 shown in Fig. 6.

q/K_F	ϵ_1	ϵ_2
0.0	10.0	0
0.1	8.0	2.0
0.4	2.1	2.3
0.9	0.3	0.76
2.0	0	0.12

For the special case of $q=0$, we get

$$\epsilon(0)=1+(\hbar\omega_p/E_g)^2[1-(E_g/4E_F)+\tfrac{1}{3}(E_g/4E_F)^2]. \tag{3.6}$$

Neglecting the small quantity E_g/E_F we have

$$\epsilon(0)\approx 1+(\hbar\omega_p/E_g)^2.$$

We now determine E_g from (3.6) by using the values $\epsilon(0)=12$ and 16 for Si and Ge, respectively, and we find that $E_g=4.8$ and 4.2 eV. These values are in good agreement with the peaks observed in the optical absorptivity,[9,10]

Phillips' suggestion that $\epsilon(\mathbf{q},\mathbf{q}+\mathbf{k})$ is in general small compared with $\epsilon(\mathbf{q},\mathbf{q})$ has been verified explicitly for our model by Wiser.[11]

IV. NUMERICAL RESULTS

We have evaluated $\epsilon(\mathbf{q})$ for Si as shown in Fig. 5. Also plotted is the simple interpolation formula

$$\epsilon(\mathbf{q})=1+(\hbar\omega_p/E_g)^2F[1+(E_F/E_g)(q/K_F)^2F^{1/2}]^{-2}, \tag{4.1}$$

where $F\equiv 1-\frac{1}{4}(E_g/E_F)\approx 1$. This formula derives from the fact that as $q\to 0$, $\epsilon(\mathbf{q})\to 1+(\hbar\omega_p/E_g)^2$ whereas for large q, the effect of E_g is negligible and

$$\epsilon(\mathbf{q})\to 1+(\hbar\omega_p/E_F)^2(K_F/q)^2.$$

From (3.1) it is seen that $\epsilon(\mathbf{q})$ is made up of contributions from two parts of the Brillouin zone (see Fig. 6); these two parts correspond to normal and Umklapp processes. For small values of q the Umklapp processes make the largest contribution to $\epsilon(\mathbf{q})$ whereas for large q, normal processes are dominant. Table I lists the contributions from each part of the zone for various values of q/K_F.

ACKNOWLEDGMENTS

I would like to thank Professor J. C. Phillips and Professor Morrel H. Cohen for suggesting the problem and for many very helpful discussions.

APPENDIX

By approximating E_4, E_5, E_6, E_7 by $E_8=(\hbar^2/2m)\times[(\mathbf{k}+\mathbf{q})^2-\mathbf{k}^2+E_g]$ we greatly ease the problem of

[9] H. R. Philipp and E. A. Taft, Phys. Rev. **109**, 762 (1958).
[10] H. R. Philipp and E. A. Taft, Phys. Rev. **120**, 37 (1960).
[11] N. Wiser (private communication).

solving for $\epsilon(\mathbf{q})$ which is now

$$\epsilon(\mathbf{q})=1+\tfrac{4}{3}(\bar{q}/\bar{E})^2[1+\tfrac{4}{3}(\bar{q}/\bar{E})^2]^{-1}(A_1+A_2+A_3+A_8), \tag{A1}$$

where $A_i=(8\pi e^2/q^2)\sum_{\mathbf{k}}(\delta_{\mathbf{k}}{}^i/E_i)$, $\bar{q}=q/K_F$, $\bar{E}=E_g/E_F$, and $\delta_{\mathbf{k}}{}^i=1$ if $\mathbf{k}$ lies in region i and is zero otherwise.

The A_i are now given by

$$A_1=\tfrac{3}{4}(\hbar\omega_p/E_F\bar{q})^2\{-1-\tfrac{1}{4}\bar{E}+(2b_2-\tfrac{1}{2})\bar{q} +[(b_0/a)+b_2a]\ln[(2+4Q)/(2+\bar{q})] -(b_1+a^2b_3)\ln[(\tfrac{1}{2}+Q)(2+\bar{q})]\}, \quad (\bar{q}<\tfrac{1}{4}\bar{E}) \tag{A2a}$$

where

$$Q=\bar{q}/\bar{E}, \quad a=1-\tfrac{1}{4}\bar{E}, \quad b_0=4+\bar{q}+[4-a^2]\bar{q}^{-1},$$

$$b_1=4+\tfrac{1}{2}\bar{q}+(6-\tfrac{1}{2}a^2)\bar{q}^{-1}, \quad b_2=1+(3/\bar{q}), \quad b_3=1/2\bar{q},$$

$$A_1=\tfrac{3}{4}(\hbar\omega_p/E_F\bar{q})^2\Big\{\tfrac{1}{4}\bar{E}+\tfrac{1}{4}(5-\tfrac{1}{8}\bar{E})Q^{-1} +(b_1+a^2b_3)\ln\left[\frac{(\frac{1}{4}+Q)(2+\bar{q}-\frac{1}{4}\bar{E})}{(\frac{1}{2}+Q)(2+\bar{q})}\right] -\left(\frac{b_0}{a}+ab_2\right)\ln\left[\frac{(\frac{1}{4}+Q)(2+\bar{q})}{(\frac{1}{2}+Q)(2+\bar{q}-\frac{1}{4}\bar{E})}\right] -c_0\ln[(\tfrac{1}{4}+Q)(2+\bar{q}-\tfrac{1}{4}\bar{E})] +(c_1/a)\ln[(\tfrac{1}{4}+Q)/(2+\bar{q}-\tfrac{1}{4}\bar{E})]\Big\}, \quad (\tfrac{1}{4}\bar{E}<\bar{q}<1-\tfrac{1}{4}\bar{E}) \tag{A2b}$$

where Qb_0, b_1, b_2, b_3, and a are defined as they were before and

$$c_1=2c_0=(1-a^2)/\bar{q},$$

$$A_2=\tfrac{3}{2}(\hbar\omega_p/\bar{q})^2(E_FE_g)^{-1}[(1-\tfrac{1}{4}\bar{E})(\tfrac{1}{2}\bar{E}-\bar{q})], \quad (\bar{q}<\tfrac{1}{4}\bar{E}) \tag{A3a}$$

$$A_2=\tfrac{3}{8}(\hbar\omega_p)^2(E_FE_g)^{-1}\bar{q}^{-3}[1-(1-\tfrac{1}{4}\bar{E})^2]^2, \quad (\tfrac{1}{4}\bar{E}<\bar{q}<1-\tfrac{1}{4}\bar{E}) \tag{A3b}$$

$$A_3=\tfrac{3}{4}(\hbar\omega_p/E_F\bar{q})^2\{-1+\tfrac{1}{4}\bar{E}-\tfrac{3}{2}\bar{q} +(1+\tfrac{1}{4}\bar{E})\ln[(2+4Q)/(2-\bar{q})] +\tfrac{1}{2}(Q^{-1}+\bar{q})\ln[(\tfrac{1}{2}+Q)(2-\bar{q})]\}, \quad (\bar{q}<\tfrac{1}{4}\bar{E}) \tag{A4a}$$

$$A_3=\tfrac{3}{2}(\hbar\omega_p/E_F\bar{q})^2\Big\{-\tfrac{1}{8}\bar{E}-\tfrac{1}{8}Q^{-1}+(1/64)Q^{-2} +(\tfrac{1}{2}+\tfrac{1}{8}\bar{E})\ln\left[\frac{(\frac{1}{2}+Q)(2-\bar{q}+\frac{1}{4}\bar{E})}{(\frac{1}{4}+Q)(2-\bar{q})}\right] -\tfrac{1}{4}(Q^{-1}+\bar{q})\ln\left[\frac{(\frac{1}{4}+Q)(2-\bar{q}+\frac{1}{4}\bar{E})}{(\frac{1}{2}+Q)(2-\bar{q})}\right] +\tfrac{1}{8}Q^{-1}(1-\tfrac{1}{8}\bar{E})\ln[(\tfrac{1}{4}+Q)(2-\bar{q}+\tfrac{1}{4}\bar{E})]\Big\}, \quad (\tfrac{1}{4}\bar{E}<\bar{q}<1-\tfrac{1}{4}\bar{E}) \tag{A4b}$$

$$A_8=\tfrac{3}{8}(\hbar\omega_p/E_F\bar{q})^2\{1+Q^{-1}[\tfrac{1}{2}-\ln(1+2Q-Q\bar{q})] +(-\tfrac{1}{2}Q^{-1}+(1-\tfrac{1}{4}Q^{-2})\bar{q}^{-1}-\tfrac{1}{4}\bar{q}) \times\ln[(2+\bar{q}+Q^{-1})/(2-\bar{q}+Q^{-1})]\}, \quad (0<\bar{q}<1-\tfrac{1}{4}\bar{E}). \tag{A5}$$

Although A_2 can be simplified somewhat by neglecting $\bar{E}$ compared to 1, this cannot be done for A_1, A_3, or A_8.